RSC Advances

ROYAL SOCIETY OF CHEMISTRY

PAPER

View Article Online
View Journal | View Issue

Cite this: *RSC Adv.*, 2023, **13**, 6481

Circular economy in hot-dip galvanizing with zinc and iron recovery from spent pickling acids†

Andrea Arguillarena, [a] María Margallo, [a] Axel Arruti-Fernández,[b] Javier Pinedo,[b] Pedro Gómez,[b] Inmaculada Ortiz [a] and Ane Urtiaga *[a]

The management of spent pickling acids (SPA) is an environmental challenge for the hot-dip galvanizing (HDG) industry. Bearing in mind its elevated content of iron and zinc, SPA can be regarded as a source of secondary materials in a circular economy approach. This work reports the pilot scale demonstration of non-dispersive solvent extraction (NDSX) in hollow fiber membrane contactors (HFMCs) to perform the selective zinc separation and SPA purification, so that the characteristics needed for use as a source of iron chloride are achieved. The operation of the NDSX pilot plant, which incorporates four HFMCs with a 80 m^2 nominal membrane area, is carried out with SPA supplied by an industrial galvanizer, and consequently technology readiness level (TRL) 7 is reached. The purification of the SPA requires of a novel feed and purge strategy to operate the pilot plant in continuous mode. To facilitate the further implementation of the process, the extraction system is formed by tributyl phosphate as the organic extractant and tap water as the stripping agent, both easily available and cost-effective chemicals. The resulting iron chloride solution is successfully valorized as a hydrogen sulfide suppressor to purify the biogas generated in the anaerobic sludge treatment of a wastewater treatment plant. Additionally, we validate the NDSX mathematical model using pilot scale experimental data, providing a design tool for process scale-up and industrial implementation.

Received 23rd December 2022
Accepted 16th February 2023

DOI: 10.1039/d2ra08195d

rsc.li/rsc-advances

Introduction

The application of circular economy (CE) strategies is increasingly promoted since they are expected to help solve the current challenge of resource depletion in the face of increasing demand for virgin materials and in turn, to minimize or avoid waste generation.[1,2] Metal recovery from waste has been one of the fields under study. This is supported by the increasing societal demand for metals, and the importance of keeping mining reserves for sustainable development.[3] Additionally, secondary sources of metals should be promoted to reduce the environmental impacts of their primary production, which is very intensive in the use of resources and energy.[4] Furthermore, waste valorization reduces the environmental impacts associated with waste management, whenever the material credits gained by the substitution of primary materials are considered in the sustainability analysis.[5]

Considering wastes as an opportunity to recover metals, spent pickling acids (SPAs) generated in the hot-dip galvanizing (HDG) process can be prospected for the application of CE in the surface treatment sector.[6] SPAs of HDG are characterized by high contents of zinc, iron and chloride, low pH, and traces of other metals such as manganese, lead, aluminum, chromium, cadmium, nickel, copper, and cobalt.[7] SPAs are classified as a hazardous waste according to the European Waste List.[8] The reference SPAs treatment consists of neutralization/precipitation and solidification/stabilization, which leads to a stabilized sludge that ends up in a landfill, a practice that implies the loss of metallic resources.[9] The recovery of zinc and iron would provide an opportunity to complement the offer of these major metals whose demand is expected to increase continuously over the 21st century.[10,11]

Several studies have assessed different methods for SPA purification with the aim of acid and/or metals recovery.[12] For example, the simultaneous recovery of hydrochloric acid and ferric chloride by vacuum distillation,[13] or as an iron precursor to prepare iron oxide nanoparticles,[14] or as precursor of iron fluoride based electrode materials in batteries.[15] The metal recovery will typically involve a combination of a separation/purification stage followed by a recovery stage.[16,17] Previous literature proposed the integration of solvent extraction (SX) for SPA purification, followed by electrowinning (EW) for zinc electrodeposition.[18,19] The zinc speciation as negative chloro-complexes in the hydrochloric acid based SPA, mostly as $ZnCl_4^{2-}$ and $ZnCl_3^-$, and iron as positive Fe^{2+} species, opens the door to the selective extraction of zinc species by means of

[a]*Chemical and Biomolecular Engineering Department, Universidad de Cantabria, Avda. De Los Castros, s.n., 39005, Santander, Spain. E-mail: urtiaga@unican.es*

[b]*Apria Systems, Parque Empresarial de Morero, Parcela P.2-12, Nave 1-Puerta 5, 39611, Guarnizo, Spain*

† Electronic supplementary information (ESI) available. See DOI: https://doi.org/10.1039/d2ra08195d

solvating agents such as tributyl phosphate (TBP).[7,20] Besides, TBP achieves high selectivity of zinc over iron and high loading capacity.[21] About the back-extraction process, tap water has proved an optimal performance for the stripping of zinc and TBP regeneration.

Membrane-based solvent extraction (MBSX) consists of using hollow fiber membrane contactors (HFMCs) to perform the non-dispersive contact between the aqueous feed phase and the organic extractant phase. The HFMC provides large ratios of mass transfer area per unit volume of equipment and facilitates the scale-up of the technology.[22] MBSX can be implemented as two different process configurations: (i) non-dispersive solvent extraction (NDSX) utilizes two HFMCs to perform the extraction and back-extraction steps, and the organic extractant flows through both modules, allowing its continuous regeneration; and (ii) emulsion pertraction technology (EPT), where an emulsion formed by the organic extractant and the stripping phase allows the extraction and back-extraction in a single HFMC.[18,23] So far, few studies have reported the scale-up of MBSX, although there are remarkable examples dealing with the separation of hexavalent chromium from aqueous effluents of the electroplating industry,[24] and the continuous regeneration of trivalent chromium passivation baths by means of the selective separation of zinc and iron cations.[25]

This work investigates the implementation of the continuous pilot scale operation of the NDSX technology, aimed at the purification of spent pickling acids of HDG. In this way, the SPA is separated into two streams, one of which is the zinc loaded stripping phase, while the other is the purified SPA consisting of a ferrous chloride ($FeCl_2$) solution. The results were evaluated through the concentration profiles of zinc, iron, chloride, and pH both in the feed and stripping phases. The most novel aspects of this work are the purge and feed strategy that enables to operate the NDSX technology in continuous mode (instead of the commonly reported batch operation), the validation of the mathematical model with experimental data at pilot scale, the strategy for minimizing water consumption, and the reuse of the recovered iron. The innovative feed and purge strategy enhances the yield of zinc extraction. The validation of the mathematical model with experimental results at the pilot scale allows having a design tool to take decisions on the size and setting of the operation variables needed for treating a given SPA composition. Additionally, this work includes an original approach to reduce the water consumption by reusing the water stream that results after zinc electrodeposition as stripping agent. Finally, the valorization of one of the secondary materials recovered is included, giving added value to the results obtained. The zinc-free purified SPA was used to substitute commercial ferric chloride ($FeCl_3$) as hydrogen sulfide suppressor in the biogas generated in the anaerobic sludge digester at a wastewater treatment plant (WWTP) located in Northern Spain.

Methodology

Spent pickling acids characterization

Samples of SPA were supplied by a hot-dip general galvanizer. The steel components, usually of large size, were introduced into the pickling baths of hydrochloric acid by direct immersion with the help of jibs and tools. The same baths were used for dezincing of tools and non-conforming galvanized components. Table 1 presents the chemical characterization of the SPA batch used in the NDSX pilot plant tests, and the methods used for the chemical analysis. SPA is an acid aqueous solution with elevated content of chloride (174 ± 3.2 g Cl^- per L), iron (88 ± 0.49 g Fe^{2+} per L) and zinc (60 ± 0.40 g Zn^{2+} per L), and traces of other metals, being manganese concentration the highest among the minor metals (0.89 ± 0.01 g L^{-1}).

Table 1 Chemical characterization of the spent pickling acid used in pilot plant experiments[a]

	Analysis method	Value	Units
pH	Portable pH-meter	$\simeq 0$	—
Free acidity	Titration with sodium carbonate	13.6 ± 0.61	g HCl per L
Chloride	Ion chromatography	174.3 ± 3.2	g L^{-1}
Fe^{2+}	UV/vis spectrometry	87.8	
Fe^{3+}		0.7	
Fe^{Total}	Microwave plasma	88.5 ± 0.49	
Zn^{Total}	atomic emission	59.5 ± 0.40	
Nickel	spectroscopy (MP-AES)	<LoQ	
Bismuth		<LoQ	
Lead		<LoQ	
Wolfram		<LoQ	
Tin		<LoQ	
Molybdenum		0.05 ± 0.01	
Manganese		0.89 ± 0.01	
Chromium		0.07 ± 0.01	
Aluminum		0.03 ± 0.01	

[a] Limit of Quantification (LoQ): 0.25 mg L^{-1}.

Description of the pilot plant integrating NDSX and EW

Fig. 1a shows a simplified flowsheet of the SPAs treatment train that integrates NDSX and EW to recover iron and zinc simultaneously. In the NDSX stage, the objective was to reduce the SPA zinc concentration while keeping the concentration of iron as close as possible to its initial value. In this way, after the NDSX step, two streams were produced, a purified SPA stream in the form of $FeCl_2$ aqueous solution, and a stripping aqueous phase loaded with zinc chloride. Next, the zinc-loaded stripping was treated before the EW stage to remove iron traces. In the EW reactor, zinc electrodeposition took place on the cathode, while chloride oxidized on the anode to form chlorine gas. Therefore, additionally to secondary zinc and iron chloride, a solution of sodium hypochlorite (NaClO) was recovered as a product of chlorine absorption.

Despite the advantages of the NDSX treatment, one concern was the water consumption used as stripping phase. Several strategies were applied during the pilot demonstration to reduce water consumption. One approach was to replace the tap water by reclaimed water. The source of such water recycling was the output stream of the EW reactor, after zinc electrodeposition (Fig. 1a). The clarified water stream leaving the EW reactor was characterized by a pH close to neutrality (5.9–6.1),

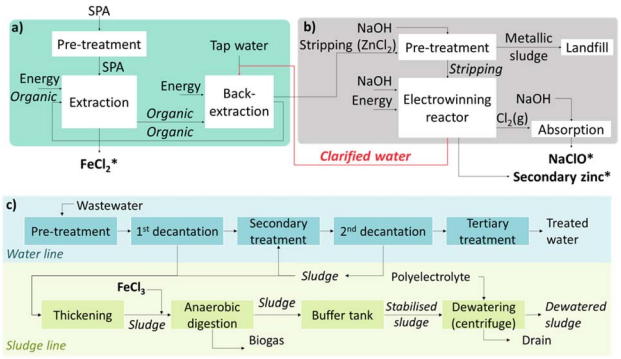

Fig. 1 Pilot plant with two integrated stages of (a) non-dispersive solvent extraction, and (b) electrowinning (*recovered products); (c) simplified diagram of a WWTP that includes sludge treatment.

zinc concentration between 1.2 and 3.8 g Zn^{2+} per L, moderate presence of chloride (18.1–22.3 g Cl^- per L), and iron concentration below the limit of quantification (<0.25 mg L^{-1}).

Feed and bleed strategy in the non-dispersive solvent extraction pilot plant for SPA purification

This section deals with the description of the NDSX stage and the feed and bleed strategy implemented for continuous operation. Fig. 2 presents the NDSX pilot plant that integrates 4

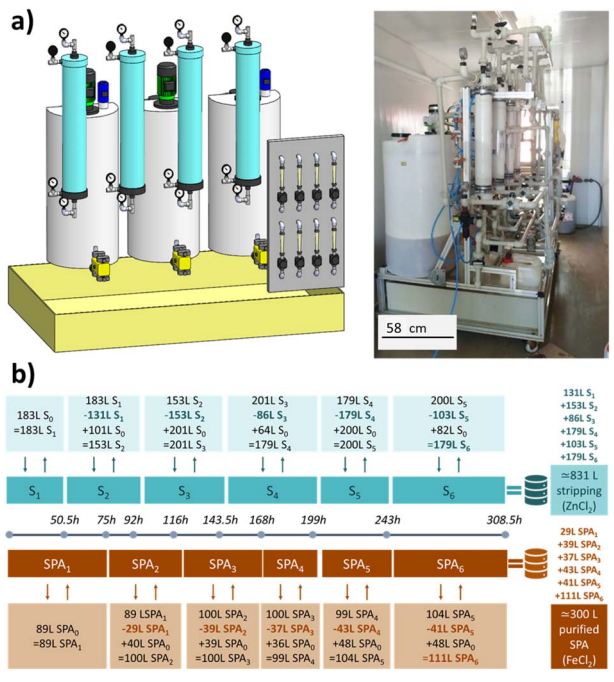

Fig. 2 (a) Non-dispersive solvent extraction pilot plant, the left side shows a schematic diagram, and the right side shows a photography of the pilot plant; (b) timeline and volumes exchanged during the feed and bleed operation of the NDSX pilot plant. The blue section represents the stripping phase, and the brown section represents the SPA phase. After 308.5 h of continuous operation, the volumes extracted from the stripping tank were mixed to form 831 L of stripping phase loaded with zinc. Similarly, the volumes extracted from the feed tank summed 300 L of purified SPA.

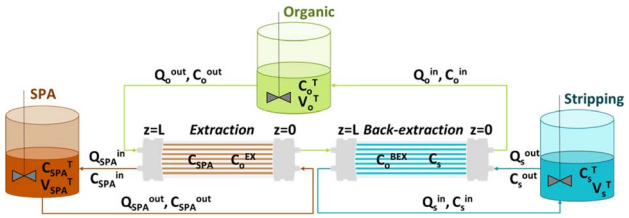

Fig. 3 NDSX system description including all variables.

microporous polypropylene HFMCs of 20 m^2 membrane area each (3 M™ Liqui-Cel™ EXF-4x28 Series). Detailed information on the HFM contactors can be found in the technical data sheets available on 3 M™ website.[26] The feed (SPA), organic and stripping phases were allocated in three independent tanks. Zinc extraction took place in two parallel HF modules, where zinc was transferred from the SPA feed phase flowing through the fibers bore, to the organic extractant phase that flowed through the shell side. In the two HFMCs used for back-extraction, zinc was transferred from the organic phase to the stripping water flowing through the inner side of the membranes. In this way, the organic phase flowed in a closed circuit that allowed its continuous regeneration. Fig. 3 describes the fluid circuits, together with the variables that will be used next in the section of mathematical modelling.

The system was equipped with filters to prevent the entry of solids in the membrane contactors and a stage of oils and fats removal. The pumping system consisted of three pneumatic double diaphragm pumps made of polypropylene and polyvinylidene fluoride. To initiate the operation, the pneumatic pumps moved the aqueous phases (feed and stripping) through the HFMCs; next, the organic phase flow started. The hydrodynamic pressure of all streams was adjusted with the back-pressure valves located at the exit of the HFMC, to achieve a minimum 0.15 bar overpressure of every aqueous stream over the organic phase flowing through the same module, at both inlet and outlet positions of each contactor. This mode of operation prevented the penetration of the organic phase into the aqueous phases and maintained the aqueous-organic interphase at the porous wall of the hydrophobic polypropylene membranes. Experiments were performed at room temperature. Two flowmeters were installed at the inlet of each HFMC.

Fig. 2b describes the feed and bleed strategy that was implemented to operate the NDSX pilot plant in continuous mode. The timeline indicates the time spots in which volume exchanges of the different liquid phases were carried out. Initially, the feed tank contained 89 L of SPA with a composition of 59.5 ± 0.40 g Zn^{2+} per L, 88.5 ± 0.49 g Fe^{2+} per L and 174.3 ± 3.2 g Cl^- per L (Table 1). In the organic tank, 185 L of organic phase formed by 50% (v/v) of TBP diluted in Shellsol D70 (aliphatic solvent) were loaded. The volume ratio between the organic (V_{ORG}) and feed (V_{SPA}) phases was fixed at $V_{ORG}/V_{SPA} = 2$ based on previous research at laboratory scale.[27] And finally, 183 L of tap water were used as the initial stripping volume. Every certain period, a part of the stripping phase was replaced

by fresh water, with the objective of reducing zinc concentration in the stripping phase, and thus increasing the driving force of zinc transfer between the feed SPA and the stripping phase. During the period S_1, the volume S_0 of stripping phase (initially fresh tap water) was maintained at 183 L. At time 50.5 h, 131 L of stripping phase (loaded with zinc) were removed from the stripping tank, and 101 L of fresh water were added, resulting in a volume of 153 L of stripping phase during the period S_2. Similarly, during the period SPA_1, the initial 89 L of feed SPA were being recirculated to the feed tank. Only when zinc concentration in the feed tank was sufficiently low, the purified SPA was partially substituted by untreated SPA. At time 75 h, 29 L of purified SPA were removed and 40 L of untreated SPA were added to the SPA feed tank, totalizing 100 L of SPA in the feed tank during the period SPA_2. This procedure of loading untreated SPA and water, as well as discharging treated SPA and loaded stripping phase was repeated in each period indicated in Fig. 2b. After 308.5 h of continuous operation, the volumes extracted from the stripping tank were mixed to form 831 L of stripping phase loaded with zinc. Similarly, the volumes extracted from the feed tank summed 300 L of purified SPA.

Mathematical model of zinc separation from SPAs in NDSX

The mathematical model of the NDSX pilot plant separation of zinc from SPA is described below using the variables defined in Fig. 3, and following our previous background on NDSX modelling at laboratory scale.[23] The purpose was to validate the model with pilot scale data and adjust the mass transfer parameters, if needed, for the scale-up of NDSX systems. The model includes dynamic mass balances that describe the evolution of zinc concentration with time in the mixing tanks, and along the axial position in the HFMC. The relevant assumptions were: (i) perfect mixing conditions in the feed, organic, and stripping tanks, (ii) plug flow for the circulation of the three fluids in the HFMC, (iii) the change of concentration along the axial position of the HFMC is much larger than the change of concentration with time, (iv) there is chemical equilibrium of zinc species at the aqueous-organic interfaces, and (v) the main resistance to mass transfer is due to diffusion of the TBP-zinc chloride complex through the organic phase that is embedded in the pores of the hollow fiber membrane wall.

- Zinc mass balances in the recirculation tanks:

$$\text{Feed tank } V_{SPA}\frac{dC_{SPA}{}^{T}}{dt} = Q_{SPA}\left(C_{SPA}{}^{in} - C_{SPA}{}^{out}\right) \quad (1)$$

$$\text{Organic tank } V_{O}\frac{dC_{o}{}^{T}}{dt} = Q_{o}\left(C_{o}{}^{in} - C_{o}{}^{out}\right) \quad (2)$$

$$\text{Stripping tank } V_{S}\frac{dC_{s}{}^{T}}{dt} = Q_{s}\left(C_{s}{}^{in} - C_{s}{}^{out}\right) \quad (3)$$

- Zinc mass balances in the extraction HFMCs:

$$\text{Feed phase } -Q_{SPA}L^{EX}\frac{dC_{SPA}}{dz} = A^{EX}\ J^{EX} \quad (4)$$

$$\text{Organic phase } -Q_{o}L^{EX}\frac{dC_{o}{}^{EX}}{\partial z} = A^{EX}\ J^{EX} \quad (5)$$

- Zinc mass balances in the back-extraction HFMCs:

$$\text{Stripping phase } Q_{s}L^{BEX}\frac{dC_{s}}{\partial z} = A^{BEX}\ J^{BEX} \quad (6)$$

$$\text{Organic phase } Q_{o}L^{BEX}\frac{dC_{o}{}^{BEX}}{\partial z} = A^{BEX}\ J^{BEX} \quad (7)$$

The zinc flux through the membrane can be described using mass transfer coefficients, as in eqn (8) and (9):

$$\text{Extraction flux } J^{EX} = k_{m}{}^{EX}\left(C_{o,i}{}^{EX} - C_{o}{}^{EX}\right) \quad (8)$$

$$\text{Back-extraction flux } J^{BEX} = k_{m}{}^{BEX}\left(C_{o}{}^{BEX} - C_{o,i}{}^{BEX}\right) \quad (9)$$

$$k_{m} = \frac{D_{i,B}\cdot\varepsilon}{\delta\cdot\tau} \quad (10)$$

$$H_{EX} = \frac{C_{o,i}{}^{EX}}{C_{SPA}} \quad (11)$$

$$H_{BEX} = \frac{C_{s}}{C_{o,i}{}^{BEX}} \quad (12)$$

The mass transfer coefficient of the zinc chloride-TBP complex (k_m) was calculated using mass transfer fundamentals, eqn (10), where the diffusivity of such species in the organic phase that embedded the porous membrane ($D_{i,B}$) was calculated using the Wilke–Chang equation.[28] The ESI† provides further information on data used for k_m calculation. The chemical equilibrium of zinc species at the interfaces was described using distribution coefficients (H_{EX}, H_{BEX}), defined in eqn (11) and (12).

Valorization of purified SPA in wastewater treatment plants

The purified SPA after NDSX was a solution of $FeCl_2$, with low zinc concentration. The valorization of the purified SPA after zinc extraction was carried out in a municipal WWTP as substitute of $FeCl_3$ solutions used to suppress hydrogen sulfide in the biogas produced. Fig. 1c presents the flowsheet of a WWTP, showing in green color the sludge line. The use of $FeCl_2$ instead of $FeCl_3$ has been reported in literature, generally showing that $FeCl_2$, alone or in combination with $FeCl_3$, is effective for reducing the presence of volatile sulfur compounds in the biogas produced in anaerobic sludge digesters,[29–31] even in studies focused on the improvement of methane (CH_4) production.[32] The $FeCl_2$ solution was used as partial substitute of the commercial $FeCl_3$ considering the normal dosing of iron at the WWTP. The variables used to measure the effect of the purified SPA on the sludge treatment were the humidity of the dewatered sludge and the composition of the biogas produced. Finally, we measured the content of heavy metals in the dewatered sludge, on dry-basis, to check its appropriateness for being used as agricultural soil amendment, according to the

limits defined in the Spanish and European Union regulations.[33,34] on the use of sewage sludge in the agricultural sector.

Results and discussion

Pilot plant results

Fig. 4a shows the evolution with time of zinc concentration along the pilot plant continuous operation with the feed and bleed strategy. The initial zinc concentration (~60 g L^{-1}) in the SPA was reduced to 1.9–4.8 g L^{-1}, at the time spots when the SPA solution was partially replaced in the feed tank (marked with vertical dotted lines). In the stripping phase, zinc concentration increased up to 23.5–37.0 g L^{-1}. In summary, around 300 L of SPA were treated using 831 L of tap water as stripping phase, in 308.5 h of continuous operation. Iron concentration in the treated SPA ranged between 74 and 91 g L^{-1}, as shown in Fig. 4b (left hand-side axis). The upper value, slightly higher than the SPA iron concentration reported in Table 1 can be explained by the capacity of TBP to transport Fe^{2+} and water, as reported by Regel-Rosocka *et al.*,[35] a factor that slightly influenced the volume of aqueous phases and metals concentrations. These data demonstrate the system capability to effectively retain iron in the feed tank, along the prolonged continuous operation period. Nonetheless, the organic phase was able to capture a small portion of iron, as this metal was detected in the stripping stream at reduced concentrations. In the last cycle, 1.1 g L^{-1} of iron were found (right hand-side axis of Fig. 4b) in the stripping phase, showing that the continuous operation with the feed and bleed strategy favored achieving low iron transfer. Most of the iron in the stripping phase was found as iron(III), in agreement with previous literature reporting the low selectivity of zinc solvating extractants over iron(III) and the much higher selectivity of this kind of reagents over iron(II).[35] This result is beneficial for the subsequent zinc recovery in the EW reactor.

Fig. 4c shows the evolution of chloride and pH in the SPA and stripping phases. The extraction and back-extraction of zinc by TBP involved the participation of both species. The transfer of chloride and protons from the SPA to the stripping phase confirmed that zinc was extracted as zinc chloro-complexes. As a result of protons mass transfer, the water used as stripping phase became more acidic and chloride enriched. Table 2 reports the chemical characterizations of the purified SPA and the zinc loaded stripping phase after mixing the volumes of SPA and stripping removed from the system. Therefore, a zinc extraction yield of 96% was reached in the treated SPA, taking as reference the initial concentration of zinc in the SPA (59.5 g L^{-1}).

One objective of the pilot scale demonstration was to reduce the water consumption used as tripping agent. To that end, Fig. 5 compares zinc extraction kinetics, using either tap water or reclaimed water as stripping agent. The clarified water stream obtained after Zn electrodeposition in the EW reactor (Fig. 1a identifies the clarified water stream) was recycled to the NDSX stage to use it as stripping agent, with the following inlet composition: 18.1 g Cl^- per L, 1.2 g Zn^{2+} per L, <0.25 mg Fe^{2+} per L, and pH 6.1. In Fig. 5, there is an overlap of the data of zinc concentration using fresh tap water and the recycled clarified water stream, indicating that the kinetics of zinc extraction and back-extraction were similar in both conditions. Therefore, this experiment demonstrated that water consumption of the NDSX stage can be largely reduced by recycling the clarified water

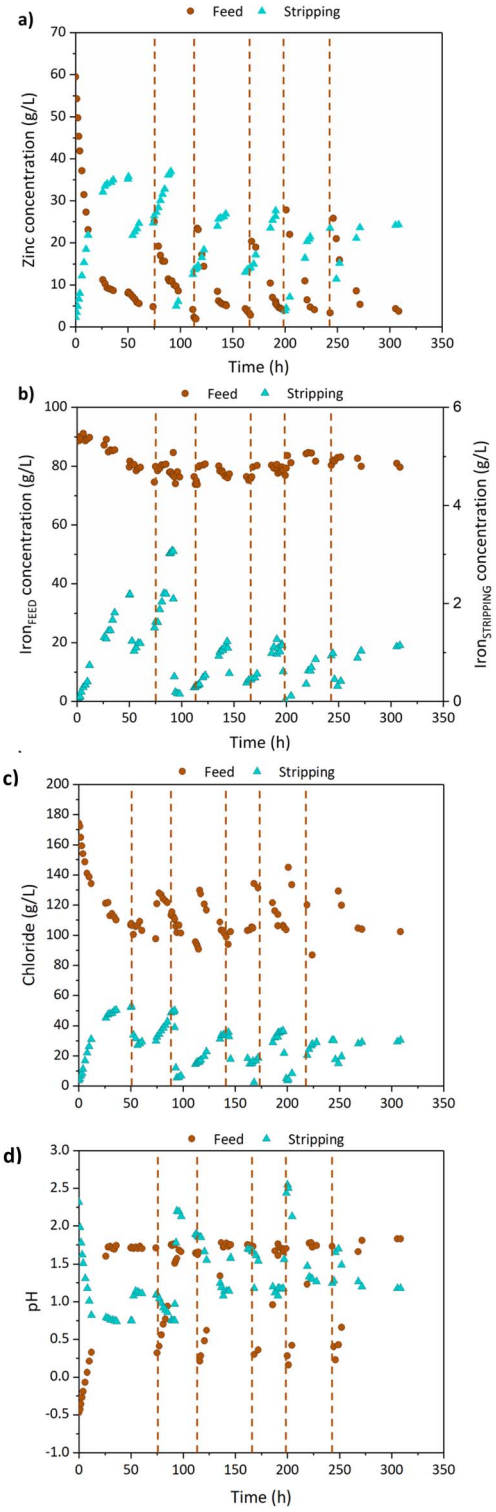

Fig. 4 (a) Zinc concentration, (b) iron concentration, (c) chloride concentration, and (d) pH in the feed (circles) and stripping tanks (triangles). The vertical dotted lines mark the time spots of exchange of treated SPA by fresh SPA.

Table 2 Characterization of purified SPA and stripping phase after mixing of extraction batches presented in Fig. 4

	Purified SPA	Stripping	Units
pH	1.9	1.1	—
Chloride	83.9	43.5	g L^{-1}
Zn	2.3	29.8	
Fe	71.7	1.5	

stream produced in the EW stage of the zinc recovery process, thus leading to a more sustainable valorization process.

Validation of the mathematical model with pilot scale experimental data

The mathematical model presented previously was used to describe the dynamic performance of zinc extraction and back-extraction in the pilot plant, using empirical data to validate the proposed model. Firstly, we calculated the mass transfer coefficient of zinc through the membrane (k_m) following the methodology detailed in the ESI.† Literature collects several studies dealing with the distribution coefficient (H_{EX}), of zinc between chloride-based SPA and TBP extractant.[36] In this work, we have selected the values reported by Mansur *et al.*,[37] as these authors considered similar SPA chemical properties to those used in the present study. The authors expressed the extraction partition coefficient as function of TBP concentration in the organic phase, that in this study was 50% v/v, equivalent to 1.8 mol L^{-1}. In this work, the distribution coefficient of the back-extraction process (H_{BEX}) was calculated as $H_{BEX} = (1/H_{EX})(C_{S,eq}/C_{SPA,eq})$, where the equilibrium concentrations of zinc in the aqueous stripping and in the organic phase in equilibrium were taken from experimental data in Fig. 6a, $C_{S,eq} = 55.7$ g L^{-1} and $C_{SPA,eq} = 23.9$ g L^{-1}. Table 3 summarizes the parameters used to simulate the pilot plant results.

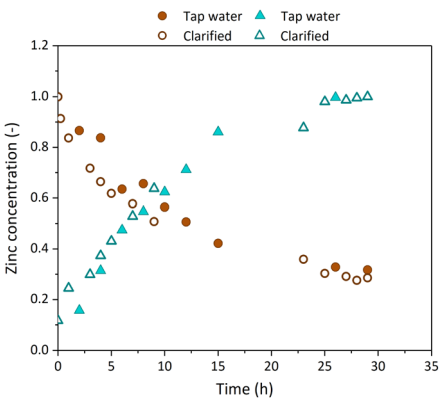

Fig. 5 Evolution with time of zinc concentration in the feed (circles) and stripping (triangles) tanks, using fresh tap water or clarified water (EW output) as stripping phase. Dimensionless concentrations refer to initial the feed concentration: 75.2 g L^{-1} using tap water and 56.4 g L^{-1} using recycled clarified water.

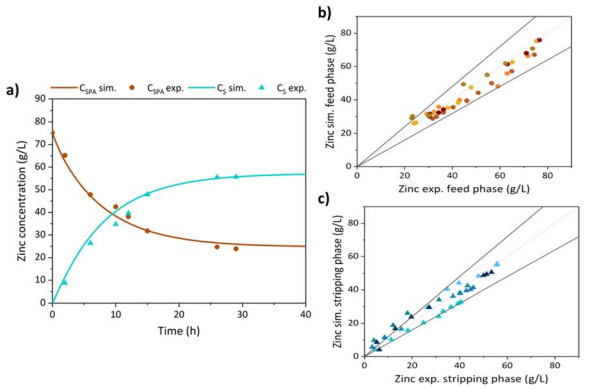

Fig. 6 (a) Simulated (solid lines) and experimental data of zinc concentration in the feed (circles) and stripping (triangles) phases. $V_{SPA} = 61$ L; $V_{ORG} = 76$ L; $V_S = 65$ L. 4 HFMCs (Liqui-Cel Extra-Flow 2.5 in x8 in) 2 HFMC in parallel for extraction, and 2 HFMC in parallel for back-extraction. The effective membrane area of the HFMC was calculated after visual inspection of the cross section and the membrane length available for mass transfer, 17.2 m^2 each module, somewhat lower than the nominal 20 m^2 reported by the manufacturer. Parity graph of simulated *vs.* experimental zinc concentrations in (b) feed tank and (c) stripping phase tank.

Table 3 Parameters of the NDSX mathematical model

Parameter	Value	Units
H_{EX}	0.36	—
H_{BEX}	6.44	—
k_m	2.45×10^{-7}	m s^{-1}

Fig. 6a shows the comparison between experimental data of the kinetic evolution of zinc in the SPA feed tank and in the stripping tank working in batch mode (data previously reported in[7]), and the simulation results achieved with the model reported in the present study, in the conditions referred in the figure caption. The good match of simulated and experimental data confirms that the model predicts satisfactorily the pilot plant performance. Finally, Fig. 6b and c present the parity graphs of experimental *versus* simulated results of five consecutive batch experiments with similar experimental conditions of those used in Fig. 6a. 95% of simulated feed concentration

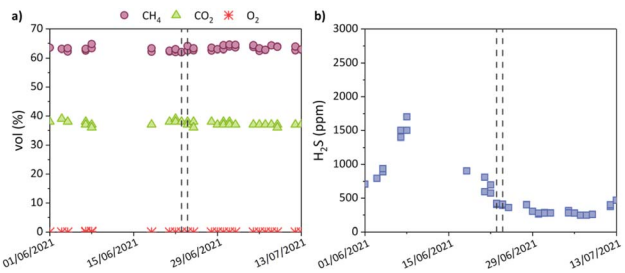

Fig. 7 Concentration of (a) CH_4, CO_2 and O_2 and (b) H_2S, in the biogas produced in the sludge digester at the WWTP. The vertical dotted lines indicate the addition of purified SPA as iron source for hydrogen sulfide suppression.

Table 4 Metals in dewatered stabilized sewage sludge

Metal	Units	Commercial $FeCl_3$ before SPA addition	Purified SPA after SPA addition	Max. limit
Cadmium	mg kg^{-1} dry matter	<LoQ	<LoQ	20
Copper		262 ± 2.2	315 ± 37	1000
Nickel		7.5 ± 2.5	10.7 ± 2.9	300
Lead		<LoQ	<LoQ	750
Zinc		734 ± 9.3	857 ± 78	2500
Mercury		<LoQ	<LoQ	16
Chromium		45.0 ± 0.04	48.6 ± 4.5	1000

values fall in the range $[Zn]_{exp}^{EX} \pm 20\%$ $[Zn]_{exp}^{EX}$, while 81% of simulated stripping concentration values fall in the range $[Zn]_{exp}^{BEX} \pm 20\%$ $[Zn]_{exp}^{BEX}$. The differences between simulated and experimental results in the stripping phase might be due to water uptake by TBP,[38] that reduced the stripping phase volume along the experimental run, a factor that increased the uncertainty of the simulations, as the change of stripping volume with time was not considered in the model.

Iron valorization. Case study of using purified SPA as source of iron chloride in a WWTP

Using the purified SPA as source of iron resulted in an excellent performance of the sewage sludge line considering the composition of the biogas produced in the anerobic sludge digester. Fig. 7 presents the biogas composition in the standard operation conditions of the anaerobic digester, and after using purified SPA as source of iron. The major components were CH_4 with an average concentration of 63.0 ± 0.8% vol., and CO_2 at 37.4 ± 1.3% vol. The concentration of O_2 was maintained at very low values. The H_2S concentration in the biogas upon addition of purified SPA stayed below 500 ppm. Meanwhile, the dewatered sludge was thoroughly characterized along a period of 3 months (1 sample per week), showing good uniformity in its main chemical parameters, *e.g.*: the average humidity was 79.2 ± 1.2%. Table 4 shows the concentration of heavy metals in the dewatered sludge, calculated as the average of 10 samples. The highest concentration was 857 ± 7.8 mg Zn per kg dry matter, meaning that the stabilized sludge generated in the WWTP was securely below the maximum limits for being used as amendment for agricultural soils (<2500 mg Zn per kg dry matter for acidic soils with pH lower than 7). The same conclusion applies for the rest of metals considered in the Spanish and European regulations.[33,34]

Conclusions

This work makes progress on the knowledge aimed at the recovery of zinc and iron resources contained in the spent pickling acids of hot dip galvanizing. The following conclusions summarize the scientific advances made to achieve this goal:

- The technical feasibility of the non-dispersive solvent extraction technology has been demonstrated at pilot scale, in a real environment and reaching a technology readiness level (TRL) 7. For that purpose, a NDSX pilot plant that incorporates 80 m^2 of membrane area in 4 membrane contactors has been successfully built and operated with real industrial SPA, allowing the selective separation of zinc with respect to divalent iron and trace metals.
- The NDSX pilot plant has been adapted to the continuous operation mode, by applying a feed and bleed strategy that enables to increase the zinc extraction yield and eventually, to obtain the purified SPA as a $FeCl_2$ solution.
- Considering the circular economy approach, the purified SPA has been valorized in a municipal wastewater treatment plant, where SPA was applied as hydrogen sulfide suppressor in the biogas produced in the anaerobic digester, whereas the stabilized sludge maintained the properties needed for its use as amendment of agricultural soil.

Overall, these findings contribute to the current knowledge related to the pilot scale technology demonstration of NDSX in hollow fiber membrane contactors, and the valorization of the secondary metal products in the context of the circular economy.

Nomenclature

V_{SPA}, V_O, V_S	Volume of SPA, organic and stripping phases in the recirculation tanks (m^3)
Q_{SPA}, Q_o, Q_s	Flow rate of SPA, organic and stripping phases (L h^{-1})
C_{SPA}^{T}, C_o^{T}, C_s^{T}	Zinc concentration in the corresponding tank (g L^{-1})
C_{SPA}^{in}, C_o^{in}, C_s^{in}	Zinc concentration in inlet streams to each tank (g L^{-1})
C_{SPA}^{out}, C_o^{out}, C_s^{out}	Zn concentration in outlet streams of tanks (g L^{-1})
C_{SPA}, C_s	Bulk concentration in the SPA and stripping phases (g L^{-1})
$C_{o,i}^{EX}$, $C_{o,i}^{BEX}$	Interfacial concentration in the organic phase, in the extraction and back-extraction modules (g L^{-1})
C_o^{EX}, C_o^{BEX}	Bulk concentration in the organic phase in the extraction and back-extraction modules (g L^{-1})
J^{EX}, J^{BEX}	Solute flux of extraction and back-extraction (g h^{-1} L^{-1})
k_m^{EX}, k_m^{BEX}	Mass transfer coefficients in the extraction and back-extraction modules (m h^{-1})

A^{EX}, A^{BEX}	Extraction and back-extraction membrane area (m^2)
L^{EX}, L^{BEX}	Length of hollow fibre contactor for extraction and back-extraction (m)
$D_{i,B}$	Diffusivity of the zinc chloride organic complex $\overline{ZnCl_2 \cdot 2HCl \cdot 4TBP}$ in the organic extractant phase ($m^2\ h^{-1}$)
ε	Porosity of the membrane (−)
δ	Thickness of the membrane (m)
τ	Tortuosity of the membrane (−)

Author contributions

Conceptualization, AU and IO; methodology, AU, PG, AA and MM; investigation, AA and AAF; writing—original draft preparation, AA; writing—review and editing, AU and IO; project administration, AU and JP; funding acquisition, AU, PG and JP. All authors have read and agreed to the published version of the manuscript.

Conflicts of interest

There are no conflicts to declare.

Acknowledgements

This research was co-funded by the European LIFE Program, project LIFE2ACID Towards a sustainable use of metal resources in the galvanic industry, grant number LIFE 16 ENV/ES/000242. The authors are grateful to Julia Beleña and Eva Pozo (Galvanizadora Valenciana S. L.) for providing SPA batch samples. We also acknowledge Leandro Morante and Ana Fernández (MARE S. A.) for their assistance with the on-site tests at the WWTP dealing with the valorization of purified SPA. The research behind this paper would not have been possible without the participation of Isabel Ortiz, Germán Santos, and Andrés del Castillo (APRIA Systems S. L.) in the operation of the pilot plant.

Notes and references

1 P. Schröder, A. Lemille and P. Desmond, *Resour., Conserv. Recycl.*, 2020, **156**, 104686.
2 W. Hagedorn, S. Jäger, L. Wieczorek, P. Kronenberg, K. Greiff, S. Weber and A. Roettger, *J. Cleaner Prod.*, 2022, **377**, 134439.
3 V. V. Gedam, R. D. Raut, A. B. Lopes de Sousa Jabbour and N. Agrawal, *Resour. Policy*, 2021, **74**, 102279.
4 M. R. Gorman, D. A. Dzombak and C. Frischmann, *Resour., Conserv. Recycl.*, 2022, **184**, 106424.
5 S. Shi, G. Xu, H. Yu and Z. Zhang, *J. Chem. Technol. Biotechnol.*, 2018, **93**, 936–944.
6 A. Arguillarena, M. Margallo, Á. Irabien and A. Urtiaga, *J. Environ. Manage.*, 2022, **318**, 115567.
7 A. Arguillarena, M. Margallo, A. Arruti-Fernández, J. Pinedo, P. Gómez and A. Urtiaga, *Membranes*, 2020, **10**, 444.
8 European Commission, 2014/955/EU, Commission Decision amending Decision 2000/532/EC on the list of waste pursuant to Directive 2008/98/EC, *Official Journal of the Euroepan Comission*, 2014, **L370**, 44.
9 A. Devi, A. Singhal, R. Gupta and P. Panzade, *Clean Technol. Environ. Policy*, 2014, **16**, 1515–1527.
10 M. Stasiak, M. Regel-Rosocka and A. Borowiak-Resterna, *Hydrometallurgy*, 2016, **162**, 57–62.
11 T. Watari, K. Nansai and K. Nakajima, *Resour., Conserv. Recycl.*, 2021, **164**, 105107.
12 M. Regel-Rosocka, *J. Hazard. Mater.*, 2010, **177**, 57–69.
13 C. H. Tsai, Y. H. Shen and W. Tsai, *Sustainability*, 2021, **13**, 9410.
14 D. T. Nguyen, L. T. Pham, H. T. T. Le, M. X. Vu, H. T. M. Le, H. T. M. Le, N. H. Pham and L. T. Lu, *RSC Adv.*, 2018, **8**, 19707–19712.
15 S. Sanghvi, N. Pereira, A. Halajko and G. G. Amatucci, *RSC Adv.*, 2014, **4**, 57098–57110.
16 N. Diban, R. Mediavilla, A. Urtiaga and I. Ortiz, *J. Hazard. Mater.*, 2011, **192**, 801–807.
17 V. García, P. Häyrynen, J. Landaburu-Aguirre, M. Pirilä, R. L. Keiski and A. Urtiaga, *J. Chem. Technol. Biotechnol.*, 2014, **89**, 803–813.
18 E. Bringas, M. F. San Román, A. Urtiaga and I. Ortiz, *Chem. Eng. Process.: Process Intensif.*, 2013, **67**, 120–129.
19 J. Carrillo-Abad, M. Garcia-Gabaldon, I. Ortiz-Gandara, E. Bringas, A. M. Urtiaga, I. Ortiz and V. Perez-Herranz, *Sep. Purif. Technol.*, 2015, **151**, 232–242.
20 I. Ortiz, E. Bringas, M. F. San Roman and A. Urtiaga, *Sep. Sci. Technol.*, 2004, **39**, 2441–2455.
21 R. Cierpiszewski, I. M. Miesiąç, M. Regel-Rosocka, A. M. Sastre and J. Szymanowski, *Ind. Eng. Chem. Res.*, 2002, **41**, 598–603.
22 A. I. Alonso, A. Urtiaga, S. Zamacona, A. Irabien and I. Ortiz, *J. Membr. Sci.*, 1997, **130**, 193–203.
23 A. Urtiaga, M. J. Abellán, J. A. Irabien and I. Ortiz, *J. Membr. Sci.*, 2005, **257**, 161–170.
24 Z. Zhang, H. Luo, X. Jiang, Z. Jiang and C. Yang, *RSC Adv.*, 2015, **5**, 47408–47417.
25 A. Urtiaga, E. Bringas, R. Mediavilla and I. Ortiz, *J. Membr. Sci.*, 2010, **356**, 88–95.
26 3 M™, Liqui-Cel™, *Membrane Contactors – Data Sheets*, **https://www.3m.com.es/3M/es_ES/liquicel-technology-gas-control-es/**, accessed February 15, 2023.
27 J. Laso, V. García, E. Bringas, A. Urtiaga and I. Ortiz, *Ind. Eng. Chem. Res.*, 2015, **54**, 3218–3224.
28 J. Li, L. Yang, X. Ding, J. Chen, Y. Wang, G. Luo and H. Yu, *RSC Adv.*, 2015, **5**, 79164–79171.
29 P. Jameel, *J. – Water Pollut. Control Fed.*, 1989, **61**, 230–236.
30 B. R. Dhar, E. Youssef, G. Nakhla and M. B. Ray, *Bioresour. Technol.*, 2011, **102**, 3776–3782.
31 J. Kulandaivelu, S. Shrestha, W. khan, J. Dwyer, A. Steward, L. Bell, P. Mcphee, P. Smith, S. Hu, Z. Yuan and G. Jiang, *Chemosphere*, 2020, **250**, 126221.
32 Y. Qin, L. Chen, T. Wang, J. Ren, Y. Cao and S. Zhou, *Renewable Energy*, 2019, **139**, 1290–1298.

33 Ministerio de Agricultura Pesca y Alimentación, Real Decreto 1310/1990, de 29 de octubre, por el que se regula la utilización de los lodos de depuración en el sector agrario, *Biomed. Opt. Express*, 1990, **262**, 32339.
34 European Commission, Council Directive 86/278/EEC on the protection of the environment, and in particular of the soil, when sewage sludge is used in agriculture, *Official Journal of the Euroepan Comission*, 1986, **L181**, 6.
35 M. Regel-Rosocka and J. Szymanowski, *Solvent Extr. Ion Exch.*, 2005, **23**, 411–424.
36 K. H. Lum, G. W. Stevens, J. M. Perera and S. E. Kentish, *Hydrometallurgy*, 2013, **133**, 64–74.
37 M. B. Mansur, S. D. F. Rocha, F. S. Magalhães and J. dos S. Benedetto, *J. Hazard. Mater.*, 2008, **150**, 669–678.
38 C. Xu, J. Zhou, S. Yin, Y. Wang, L. Zhang, S. Hu, X. Li and S. Li, *Sep. Purif. Technol.*, 2021, **278**, 119279.